Isolated versus Condensed Anion Structure IV:
An NQR Study and X-ray Structure Analysis of
$[H_3N(CH_2)_3NH_3]CdI_4 \cdot 2H_2O$, $[H_3CNH_2(CH_2)_3NH_3]CdBr_4$,
$[(CH_3)_4N]_2CdBr_4$, and $[(CH_3)_3S]_2CdBr_4$*

Hideta Ishihara[a], Keizo Horiuchi[b], Shi-qi Dou[c], Thorsten M. Gesing[c], J.-Christian Buhl[c], Helmut Paulus[a], and Hartmut Fuess[d]

[a] Faculty of Culture and Education, Saga University, Honjo-machi 1, Saga 840-8502, Japan
[b] College of Science, University of the Ryukyus, 1 Senbaru, Nishihara, Okinawa 903-0213, Japan
[c] Institut für Mineralogie, Universität Hannover, Welfengarten 1, D-30167 Hannover
[d] Fachbereich Materialwissenschaft, Fachgebiet Strukturforschung, Technische Universität Darmstadt, Petersenstraße 23, D-64287 Darmstadt

The phase I of $[H_3N(CH_2)_3NH_3]CdI_4 \cdot 2H_2O$ (1) crystallizes with isolated $[CdI_4]^{2-}$ tetrahedra; monoclinic, C2/c, Z = 8, a = 1702.6(3), b = 1459.3(3), c = 1555.5(3) pm, and β = 120.32(3)° at 299 K. (1) shows a first-order phase transition at $T_{I \leftrightarrow II}$ = 245 K. The eight $^{127}I(\nu_1)$ NQR lines in phase II change discontinuously into four lines in phase I. The transition entropy from DSC measurements, ΔS = 5.0 J K^{-1} mol^{-1}, shows that this transition is probably due to order-disorder of cations. $[H_3CNH_2(CH_2)_3NH_3]CdBr_4$ (2) crystallizes with isolated $[CdBr_4]^{2-}$ tetrahedra; orthorhombic P2$_1$2$_1$2$_1$, Z = 4, a = 1447.8(5), b = 1280.3(4), c = 709.7(3) pm at 299 K. (2) shows four ^{81}Br NQR lines between 77 and around 325 K, above which temperature the lines disappear. $[(CH_3)_4N]_2CdBr_4$ (3) shows a second-order phase transition at $T_{I \leftrightarrow II}$ = 271 K. Three of four ^{81}Br NQR lines in phase II disappear below this transition point, the other line can be observed up to 315 K. The transition entropy, ΔS = 9.01 J K^{-1} mol^{-1}, indicates that the transition is an order-disorder type of the cations. $[(CH_3)_3S]_2CdBr_4$ (4) shows a first-order type phase transition at $T_{I \leftrightarrow II}$ = 304 K. The four lines spectrum of ^{81}Br NQR is observed in phase II and disappears above the transition point. The transition entropy, ΔS = 46.8 J K^{-1} mol^{-1} is abnormally large. The role of the hydrogen bond and the bridging power between the halogen and cadmium atoms upon the formation of the condensed anion structure is discussed.

Introduction

We have studied the influence of the cations on the condensation of the anions in the salts (A')M^{II}Br$_4$ and (A)$_2$M^{II}Br$_4$ (M = Cd, Zn) by Br NQR and X-ray crystal structure determinations [1–3]. The role of the hydrogen bonds on the formation of the condensed anion structures is pronounced. In order to confirm this conclusion, we prepared complexes with cations without hydrogen atoms involved in hydrogen bonds or which have other groups hindering the formation of hydrogen bonds. In addition, the bridging power of the halogen ligands is also important for the formation of the complex. $[H_3N(CH_2)_3NH_3]CdX_4$ (X = Cl, Br) have layered structures [2, 4]. Therefore, we prepared the iodide analogue in order to compare the briding power. During this study the phase transitions of the title compounds were ob-

served. We report here the NQR results of these four compounds and the crystal structures of $[H_3N(CH_2)_3NH_3]CdI_4 \cdot 2H_2O$ and $[H_3CNH_2(CH_2)_3NH_3]CdBr_4$.

Experimental

The title compounds were synthesized from 1,3-propanediamine, N-methyl-1,3-propanediamine, tetramethylammonium bromide, trimethylsulphonium bromide, CdCO$_3$, and HI or HBr. The components were mixed in stoichiometric ratio in a solution of HI or HBr at pH < 3. The solvents were withdrawn by P$_2$O$_5$ in a desiccator. The results of the chemical analyses (in weight %, found/calculated) are as follows: (1): C, 4.95/4.92; H, 2.07/2.20; N, 3.79/3.82. (2): C, 9.00/9.20; H, 2.66/2.70; N, 5.17/5.36. (3): C, 16.17/16.55; H, 4.14/4.16; N, 4.62/4.82. (4): C, 12.26/12.29; H, 3.15/3.09; N, 0.02/0.00. Small single crystals for the X-ray diffraction experiments were grown from aqueous solutions. The structures were determined using a four circle X-ray diffractometer (Stoe-Stadi 4).

---

* Presented at the XIth NQI International Symposium.

Reprint requests to Prof. H. Ishihara;
E-mail: ishihara@cc.saga-u.ac.jp

Table 1. Experimental conditions for the crystal structure determinations and crystallographic data of 1,3-propanediammonium tetraiodocadmate(II) dihydrate, $[H_3N(CH_2)_3NH_3]CdI_4 \cdot 2H_2O$ (**1**) and N-methyl-1.3-propanediammonium tetrabromocadmate(II) $[H_3CNH_2(CH_2)_3NH_3]CdBr_4$ (**2**). Diffractometer: Stoe-Stadi 4; wavelength: 71.069 pm (MoKα); Monochromator: Graphite (002); scan $2\omega/\theta$. (**1**): $C_3H_{16}CdI_4N_2O$, $M = 732.20$, (**2**): $C_4H_{14}Br_4CdN_2$, $M = 522.20$

Compound	(1)	(2)
Crystal size/(mm)^3	$0.68 \times 0.72 \times 0.65$	$6.00 \times 0.52 \times 0.17$
Temperature/K	299(2)	299(2)
Absorption coeff./m^{-1}	8700	13422
θ-range for data collected	$2.00 \le \theta/° \le 28.08$	$2.12 \le \theta/° \le 25.00$
Index ranges	$-18 \le h \le 22$	$-17 \le h \le 17$
	$-17 \le k \le 19$	$-15 \le k \le 10$
	$-20 \le l \le 20$	$0 \le l \le 8$
Lattice constants		
a/pm	1702.6(3)	1447.8(5)
b/pm	1459.3(3)	1280.3(4)
c/pm	1555.5(3)	709.7(3)
$\alpha/°$	90.00	90.00
$\beta/°$	120.32(3)	90.00
$\gamma/°$	90.00	90.00
$V \cdot 10^{-6}/(pm)^3$	3336.17(9)	1315.5(8)
Space group	$C_{2h}^6 - C2/c$	$D_2^4 - P2_12_12_1$
Formula units Z	8	4
$\rho_{calc}/(Mg \cdot m^{-3})$	2.987(2)	2.637(2)
$F(000)$	2672.0	960.0
Reflections collected	22279	4689
Symmetry independent	3998	2325
$[R_{int}]$	0.08	0.0410
Data $(F_0 > 4\sigma(F_0))$	2306	2325
Restraints/Parameters	0/129	0/103
Goodness of fit on F^2	0.610	1.059
Final R $(F_0 > 4\sigma(F_0))$	$R_1 = 0.0325$,	$R_1 = 0.0737$
	$wR_2 = 0.0822$	$wR_2 = 0.1896$
R (all data)	$R_1 = 0.0590$,	$R_1 = 0.0770$,
	$wR_2 = 0.1081$	$wR_2 = 0.1896$
Flackparameter	–	0.01(3)
Largest diff: (peak, hole)/ $(10^{-6}e(pm)^3)$	1.2(2) and –0.8(2)	3.48 and –3.22
Extinction coeff.	0.0133(7)	0.0038(8)
Point positions:	C_2, C_4 atoms are in 4e, and others in 8f	all atoms are in 4a

Table 2. Atomic coordinates and equivalent isotropic displacement parameters U_{eq} (in pm^2) for $[H_3N(CH_2)_3NH_3]CdI_4 \cdot 2H_2O$ (**1**) and $[H_3CNH_2(CH_2)_3NH_3]CdBr_4$ (**2**). U_{eq} is defined as one third of the trace of the orthogonalized tensor U_{ij}. The temperature factor has the form: $T = \exp\{-2\pi^2(U_{11}h^2a^{*2} + U_{22}k^2b^{*2} + U_{33}l^2c^{*2} + 2U_{12}kha^*b^* + 2U_{13}hla^*c^* + 2U_{23}klb^*c^*)\}$. Atomic coordinates of hydrogen atoms are given elsewhere [6].

Atom	x	y	z	U_{eq}
$[H_3N(CH_2)_3NH_3]CdI_4 \cdot 2H_2O$ (**1**)				
Cd	0.20368(4)	0.76421(4)	0.18180(5)	436(2)
I$^{(1)}$	0.20316(4)	0.57239(4)	0.17276(5)	482(2)
I$^{(2)}$	0.34090(4)	0.82221(4)	0.14840(5)	495(2)
I$^{(3)}$	0.03327(4)	0.83121(4)	0.04123(5)	592(2)
I$^{(4)}$	0.23652(5)	0.80041(4)	0.37071(5)	551(2)
O$^{(1)}$	0.0246(4)	0.3939(4)	0.0826(5)	583(16)
O$^{(2)}$	0.2557(5)	0.5569(4)	0.4302(5)	612(17)
N$^{(1)}$	0.1396(5)	0.9302(5)	–0.0831(5)	538(19)
N$^{(2)}$	0.4227(5)	0.9423(5)	0.5671(6)	653(23)
C$^{(1)}$	0.4315(6)	0.5177(6)	0.1654(8)	616(25)
C$^{(2)}$	0.5000	0.5741(8)	0.2500	511(31)
C$^{(3)}$	–0.0332(6)	0.6138(5)	0.1577(7)	484(22)
C$^{(4)}$	0.0000	0.5605(7)	0.2500	410(26)
$[H_3CNH_2(CH_2)_3NH_3]CdBr_4$ (**2**)				
Cd	0.57354(6)	0.30352(8)	0.87714(14)	406(3)
Br$^{(1)}$	0.5844(1)	0.1033(1)	0.9152(3)	589(5)
Br$^{(2)}$	0.4124(1)	0.3544(1)	1.0065(2)	455(4)
Br$^{(3)}$	0.5936(1)	0.3526(1)	0.5276(2)	464(4)
Br$^{(4)}$	0.7111(1)	0.3896(1)	1.0521(2)	443(4)
N$^{(1)}$	0.9017(9)	0.4102(11)	0.7916(18)	507(29)
C$^{(1)}$	0.9455(9)	0.3685(13)	0.6161(24)	517(36)
C$^{(2)}$	0.8749(10)	0.3327(12)	0.4699(25)	493(33)
C$^{(3)}$	0.8316(10)	0.2261(11)	0.5195(22)	467(33)
N$^{(2)}$	0.7683(7)	0.1947(8)	0.3668(17)	292(22)
C$^{(4)}$	0.7202(10)	0.0946(10)	0.4046(22)	455(31)

heating rate 2–10 K min^{-1} with flowing dry N$_2$ gas at 40 ml min^{-1}.

Results and Discussion

$[H_3N(CH_2)_3NH_3]CdI_4 \cdot 2H_2O(1)$

1,3-propanediammonium tetraiodocadmate(II) dihydrate (**1**) crystallizes at room temperature monoclinic with C_{2h}^6-C2/c; the lattice constants etc. are listed in Table 1 [6]. Table 2 lists the positional coordinates, and equivalent isotropic thermal parameters U_{eq}. Intramolecular distances and angles of the anions are given in Table 3. In Fig. 1 the formula unit is drawn with the numbering of the atoms and the thermal ellipsoids. Figure 2 shows the projection of the unit cell onto the *ab* plane. The $[CdI_4]^{2-}$ tetrahedron in (**1**) is isolated with small dif-

From the measured intensities, corrected for Lorentz-polarization and absorption factors, the structures were determined by direct methods, Fourier syntheses, and least squares analysis with the programs given in [5]. The ^{127}I and ^{81}Br NQR spectra were recorded by an NQR spectrometer working in the superregenerative mode. DSC was carried out above 130 K with a differential scanning calorimeter DSC220 from Seiko Instruments Inc. under the following conditions: sample weight ca. 10 mg, the
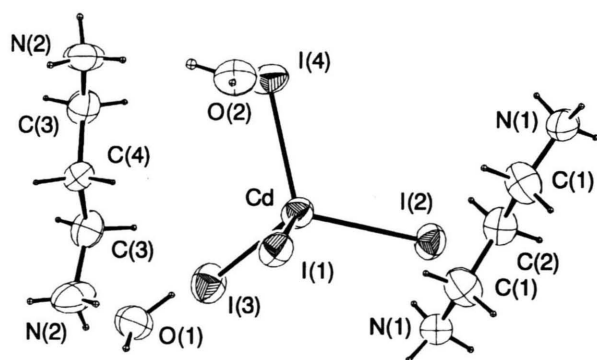
Fig. 1. Formula unit of 1,3-propanediammonium tetraiodocadmate (II) dihydrate (1) with numbering of the atoms. Cations are shown as a whole molecule. The thermal ellipsoids (50% electrons as contour) are shown, too.

ferences in the cadmium-iodine distances, $277.0 \le d$ (Cd-I)/pm ≤ 280.3 (mean value 277.7 pm), and the angles in the tetrahedron show small variations, $103.8 \le \angle$(I-Cd-I)/° ≤ 114.0 (mean value 109.4°) as shown in Table 3. The carbon atoms at the center of each 1,3-propanediammonium cation in (1) are located on the 2-fold symmetry. Intramolecular distances and angles in the cations are listed in Table 4. The distances d(N-C) are 145.5 and 146.7 pm, and d(C-C) 147.1 and 149.0 pm. $[CdI_4]^{2-}$ anion layers are on the *ac* planes situated at $b = 0.25$ and 0.75. Between these layers cations and water molecules are located. Although the N-H and O-H bond distances are fixed at 86 and 95 pm in the refinement, the angles of the N-H···I and O-H···I hydrogen bonds in (1) are listed in Table 3, in consideration of the van der Waals radii of the NH_4^+ group, the H atom, and the I atom, 160, 120, and 198 pm, respectively [7]. Two N···I hydrogen bonds, N(1)···I(1′) and N(1)···I(3), and one O···I hydrogen bond, O(1)···I(3′), are formed as shown in Figure 2. Two H_2O molecules are also involved in a series of intermolecular hydrogen bonds (see Table 3). Especially the $H_2O^{(2)}$ molecule is located between two ammonium groups, $N^{(1)}H_3^+$ and $N^{(2)}H_3^+$ groups, and then $H_2O^{(2)}$ is involved in unique hydrogen bonds.

$[N_3CNH_2(CH_2)_3NH_3]CdBr_4$ (2)

N-methyl-1,3-propanediammonium tetrabromocadmate (2) crystallizes at room temperature orthorhombic D_2^4-$P2_12_12_1$; the lattice constants etc. are listed in Table 1. Figure 3 shows the formula unit with numbering of atoms and thermal ellipsoids. Figure 4 shows the projections along [001] on to the *ab* plane. The $[CdBr_4]^{2-}$

Table 3. Intramolecular bond distances (in pm) and bond angles (in degree) for the tetrahedral coordinated CdI_4^{2-} and $CdBr_4^{2-}$ anions, and hydrogen bond scheme.

$[H_3N(CH_2)_3NH_3]CdI_4 \cdot 2H_2O$ (1)

Connection	d/pm	Connection	Angle/°
Cd-I$^{(1)}$	280.3(1)	I$^{(1)}$-Cd-I$^{(2)}$	106.11(3)
Cd-I$^{(2)}$	277.0(1)	I$^{(1)}$-Cd-I$^{(3)}$	109.62(3)
Cd-I$^{(3)}$	278.4(1)	I$^{(1)}$-Cd-I$^{(4)}$	103.84(3)
Cd-I$^{(4)}$	275.1(1)	I$^{(2)}$-Cd-I$^{(3)}$	112.87(3)
		I$^{(2)}$-Cd-I$^{(4)}$	113.95(4)
		I$^{(3)}$-Cd-I$^{(4)}$	109.92(4)

Hydrogen bond scheme

D-H···A	d(H···A)/pm	d(D···A)/pm	Angle (D-H···A)/°
O$^{(1)}$-H$^{(O1,1)}$···I$^{(3′)}$	274.1	368.2	170.2
N$^{(1)}$-H$^{(N1,2)}$···I$^{(1′)}$	298.4	358.9	126.9
N$^{(1)}$-H$^{(N1,3)}$···I$^{(3)}$	267.0	355.5	173.0
N$^{(1)}$-H$^{(N1,1)}$···O$^{(2′)}$	198.1	282.3	157.3
N$^{(2)}$-H$^{(N2,2)}$···O$^{(2″)}$	226.0	305.9	149.3
N$^{(2)}$-H$^{(N2,3)}$···O$^{(1″)}$	226.6	297.1	136.0
N$^{(2)}$-H$^{(N2,1)}$···O$^{(1‴)}$	200.1	289.0	171.6

I$^{(3′)}$: $-x$, $1-y$, $-z$; I$^{(1′)}$: $1/2-x$, $3/2-y$, $-z$; O$^{(2′)}$: $1/2-x$, $1/2+y$, $1/2-z$; O$^{(2″)}$: $1/2-x$, $1/2+y$, $1/2-z$; O$^{(1″)}$: $1/2-x$, $1/2+y$, $1/2-z$; O$^{(1‴)}$: $1/2+x$, $3/2-y$, $1/2+z$.

$[H_3CNH_2(CH_2)_3NH_3]CdBr_4$ (2)

Connection	d/pm	Connection	Angle/°
Cd-Br$^{(1)}$	258.3(2)	Br$^{(1)}$-Cd-Br$^{(2)}$	105.52(6)
Cd-Br$^{(2)}$	259.0(2)	Br$^{(1)}$-Cd-Br$^{(3)}$	109.63(6)
Cd-Br$^{(3)}$	257.6(2)	Br$^{(1)}$-Cd-Br$^{(4)}$	108.96(7)
Cd-Br$^{(4)}$	259.3(2)	Br$^{(2)}$-Cd-Br$^{(3)}$	112.44(4)
		Br$^{(2)}$-Cd-Br$^{(4)}$	114.53(6)
		Br$^{(3)}$-Cd-Br$^{(4)}$	105.72(6)

Hydrogen bond scheme

D-H···A	d(H···A)/pm	d(D···A)/pm	Angle (D-H···A)/°
N$^{(1)}$-H$^{(N1,2)}$···Br$^{(4)}$	272.3	333.2	126.7
N$^{(1)}$-H$^{(N1,3)}$···Br$^{(4′)}$	263.9	348.2	158.2
N$^{(1)}$-H$^{(N1,1)}$···Br$^{(1′)}$	255.1	337.1	153.4
N$^{(2)}$-H$^{(N2,1)}$···Br$^{(2′)}$	247.7	343.0	167.7
N$^{(2)}$-H$^{(N2,2)}$···Br$^{(3)}$	261.5	343.2	142.1

Br$^{(1′)}$: $x+1/2$, $-y+1/2$, $-z+2$; Br$^{(2′)}$: $x+1/2$, $-y+1/2$, $-z+1$; Br$^{(4′)}$: $-x+3/2$, $-y+1$, $z-1/2$.

tetrahedron in (2) is isolated with small differences in the cadmium-bromine distances, $257.6 \le d$(Cd-Br)/pm ≤ 259.3 (mean value 258.6 pm), and the angles in the tetrahedron show small variations, $105.5 \le \angle$(Br-Cd-Br)/° ≤ 112.4 (mean value 109.5°) as shown in Table 3. Intramolecular distances and angles in the cations are listed in Table 4. The distances d(N-C) are 148 and 150 pm,
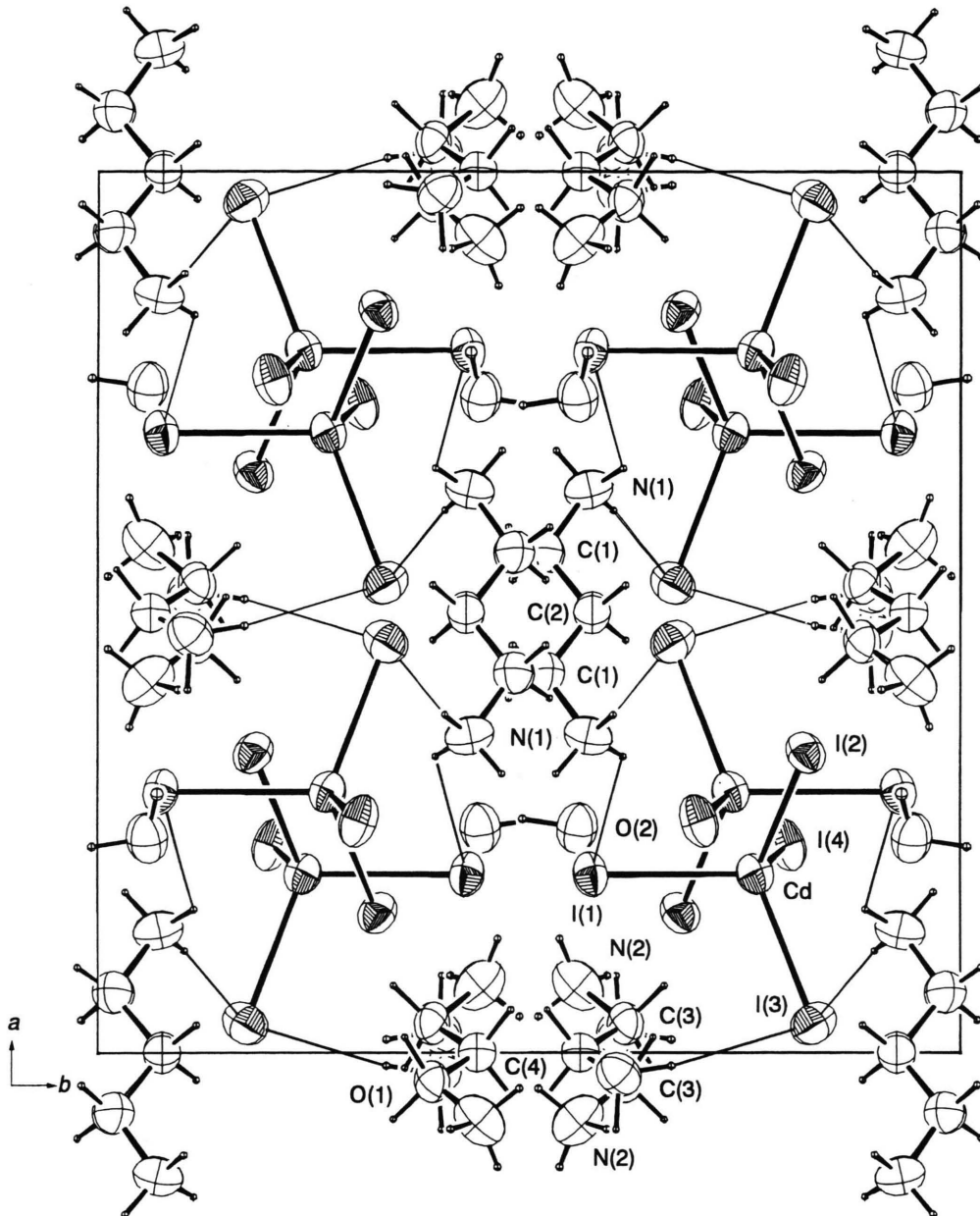
Fig. 2. Projection of the unit cell of (**1**) along [001] onto the *ab* plane. Hydrogen bonds including the I atoms are shown by thin lines.

and d(C-C) 153 and 154 pm. The torsion angle of $N^{(1)}$-$C^{(1)}$-$C^{(2)}$-$C^{(3)}$, −76.8°, is strangely small (on the other hand the torsion angles of $C^{(1)}$-$C^{(2)}$-$C^{(3)}$-$N^{(2)}$ is −177.0°). This distortion is due to the molecular packing, because the MO calculation shows the most stable conformation of the $[H_3CNH_2(CH_2)_3NH_3]^{2+}$ ion as all *anti* [8]. In Ta-

ble 3, distances and angles of the N-H···Br hydrogen bonds in (**1**) are listed in consideration of the van der Waals radii of the NH_4^+ group and the Br atom, 160 pm and 190 pm, respectively [7]. The $N^{(2)}H_2$ group forms only two hydrogen bonds of $N^{(2)}$···$Br^{(2')}$ and $N^{(2)}$···$Br^{(3)}$ because of the hindrance of the $C^{(4)}H_3$ group. The hydro-
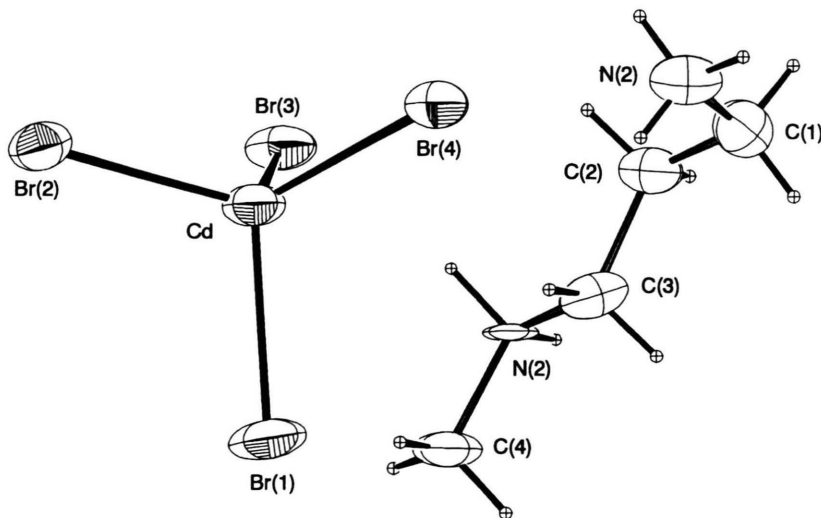
Fig. 3. Formula unit of N-methyl-1,3-propanediammonium tetrabromocadmate(II) (**2**) with the numbering of the atoms. The thermal ellipsoids (50% electrons as contour) are shown, too.

Table 4. Intramolecular distances (in pm) and angles (in degree) within the cations.

$[H_3N(CH_2)_3NH_3]CdI_4 \cdot 2H_2O$ (**1**)

Connection	d/pm	Connection	Angle/°
$N^{(1)}$-$C^{(1)}$	145.5(11)	$N^{(1)}$-$C^{(1)}$-$C^{(2)}$	114.9(7)
$N^{(2)}$-$C^{(3)}$	146.7(11)	$N^{(2)}$-$C^{(3)}$-$C^{(4)}$	113.7(7)
$C^{(1)}$-$C^{(2)}$	149.0(11)	$C^{(1)}$-$C^{(2)}$-$C^{(1')}$	113.0(11)
$C^{(3)}$-$C^{(4)}$	147.1(11)	$C^{(3)}$-$C^{(4)}$-$C^{(3')}$	116.3(11)

$C(1')$: $1-x, y, 1/2-z$
$C(3')$: $-x, y, 1/2-z$

$[H_3CNH_2(CH_2)_3NH_3]CdBr_4$ (**2**)

Connection	d/pm	Connection	Angle/°
$N^{(1)}$-$C^{(1)}$	150(2)	$N^{(1)}$-$C^{(1)}$-$C^{(2)}$	112.9(11)
$C^{(1)}$-$C^{(2)}$	153(2)	$C^{(1)}$-$C^{(2)}$-$C^{(3)}$	112.5(14)
$C^{(2)}$-$C^{(3)}$	154(2)	$C^{(2)}$-$C^{(3)}$-$N^{(2)}$	109.0(12)
$C^{(3)}$-$N^{(2)}$	148(2)	$C^{(3)}$-$N^{(2)}$-$C^{(5)}$	113.2(11)
$N^{(2)}$-$C^{(4)}$	148(2)		

Table 5. ^{127}I and ^{81}Br NQR frequencies at several temperatures for title compounds.

Compounds		T/K	v/MHz	T/K	v/MHz
$[H_3N(CH_2)_3NH_3]CdI_4 \cdot 2H_2O$ (**1**)		77	v_1[a] 83.335	277	v_1 81.699
		77	v_1 80.905	277	v_1 78.545
		77	v_1 80.328	277	v_1 76.248
		77	v_1 79.135	277	v_1 67.336
		77	v_1 76.943		
		77	v_1 76.787		
		77	v_1 74.916		
		77	v_1 71.877		
		77	v_2[a] 165.435	294	v_2 162.206
		77	v_2 157.361	294	v_2 156.429
		77	v_2 156.448	294	v_2 151.013
		77	v_2 153.313	294	v_2 128.604
		77	v_2 150.728		
		77	v_2 150.234		
		77	v_2 141.438		
		77	v_2 138.109		
$[H_3CNH_2(CH_2)_3NH_3]CdBr_4$ (**2**)		77	65.784	277	63.516
		77	60.823	277	60.224
		77	60.311	277	59.918
		77	59.130	277	57.484
$[(CH_3)_4N]_2CdBr_4$ (**3**)		77	79.920[b]	279	76.000
		77	79.920[b]		
		77	78.480		
		77	73.921		
$[(CH_3)_3S]_2CdBr_4$ (**4**)		77	68.502	277	66.246
		77	68.347	277	65.871
		77	64.232	277	61.772
		77	62.511	277	60.850

[a] v_1 and v_2 are the NQR line corresponding to the transition $m = \pm1/2 \leftrightarrow \pm3/2$ and $m = \pm3/2 \leftrightarrow \pm5/2$.
[b] a doublet.

gen bonds play an important role in the formation of the complex anions [2]. (**2**) can not form layered complex anions because of the insufficient number of the hydrogen bonds [1–3]. The hydrogen network leads to the layer structure on the *ac* plane which consists of the $[CdBr_4]^{2-}$ ions and cations as shown in Figure 4. The $N^{(1)} \cdots Br^{(4)}$ hydrogen bonds connect these layers.

Nuclear Quadrupole Resonance and Phase Transition

$[H_3N(CH_2)_3NH_3]CdI_4 \cdot 2H_2O$ (**1**) shows eight ^{127}I(v_1) NQR lines at 77 K and four lines at 277 K, as listed in

Table 5. The temperature dependence of ^{127}I(v_1) NQR frequencies is shown in Figure 5. The first-order phase transition occurs at 245 K. The eight NQR lines in phase II discontinuously change into four NQR lines in phase I at this transition point. The DSC measurement above 130 K shows the phase transition at 245 K on heat-
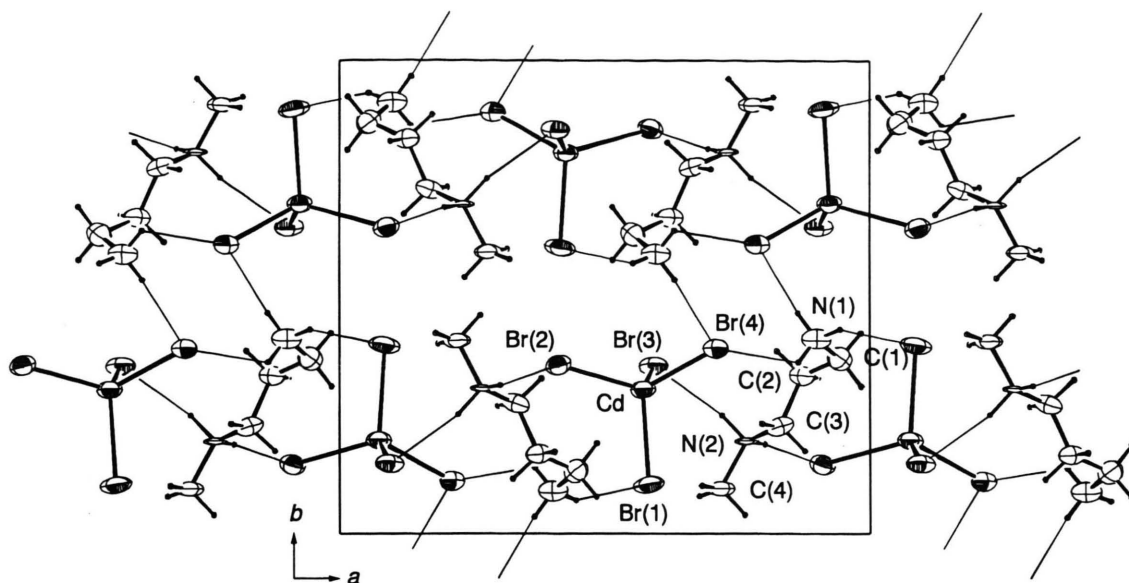
Fig. 4. Projection of the unit cell of (**2**) along [001] onto the *ab* plane. Hydrogen bonds are shown by thin lines.
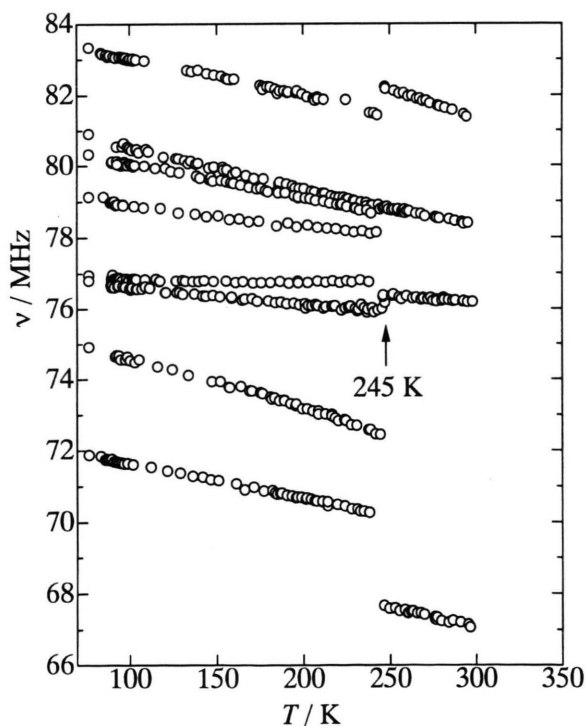

Fig. 5. Temperature dependence of $^{127}I(\nu_1)$ NQR frequencies of 1,3-propanediammonium tetraiodocadmate(II) dihydrate (**1**).

ing (the temperature hysteresis was 12 K) and the decomposition over 351 K. The transition entropy ΔS is $5.0 \ J \ K^{-1} \ mol^{-1}$ and thus is nearly $R\ln 2 = 5.8 \ J \ K^{-1} \ mol^{-1}$. Therefore, this phase transition is probably driven by a split of the cations between the two potential minima.

$[H_3CNH_2(CH_2)_3NH_3]CdBr_4$ (**2**) displays four ^{81}Br NQR lines between 77 and about 325 K, as shown in Figure 6. Four NQR lines disappear above 325 K. The DSC measurement shows no heat anomaly between 130 K and the melting point of 483 K. The disappearance of the NQR lines is probably due to the fluctuation of the electric field gradients at the Br atoms by molecular motion.

$[(CH_3)_4N]_2CdBr_4$ (**3**) exhibits four ^{81}Br NQR lines at 77 K. The temperature dependence of the ^{81}Br NQR frequencies is shown in Figure 7. A second-order phase transition occurs at 271 K, in good agreement with the result of the DTA [9] and X-ray measurements [10]. Three of the four NQR lines disappear below the transition point. The other line continuously changes at the transition point and is observed up to 315 K. This feature of the temperature dependence of the NQR frequencies is very similar to $[(CH_3)_4N]_2HgBr_4$ [11] and $[(CH_3)_4N]_2ZnBr_4$ [12], and these three compounds are isostructural. The transition entropy from the DSC measurement, $\Delta S = 9.0 \ J \ K^{-1} \ mol^{-1}$, equals almost $2R\ln 2$. Therefore we conclude that the transition is of the order-disorder type
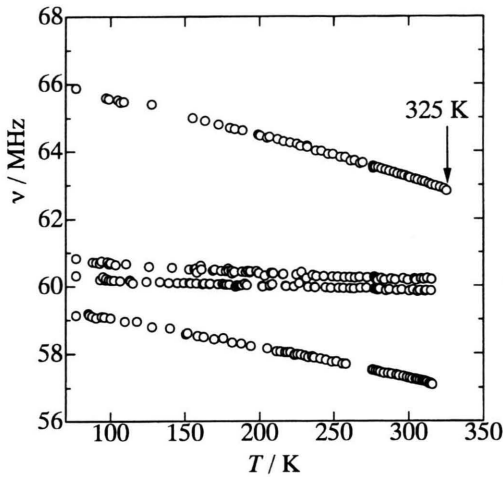
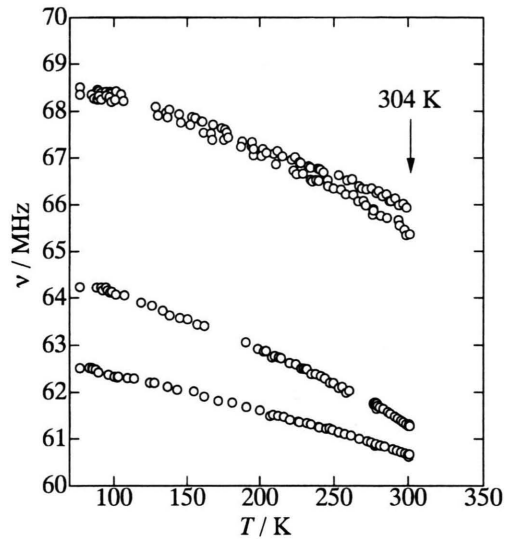Fig. 6. Temperature dependence of ^{81}Br NQR frequencies of N-methyl-1,3-propanediammonium tetrabromocadmate(II) (**2**).

Fig. 7. Temperature dependence of ^{81}Br NQR frequencies of bis(tetramethylammonium) tetrabromocadmate(II).
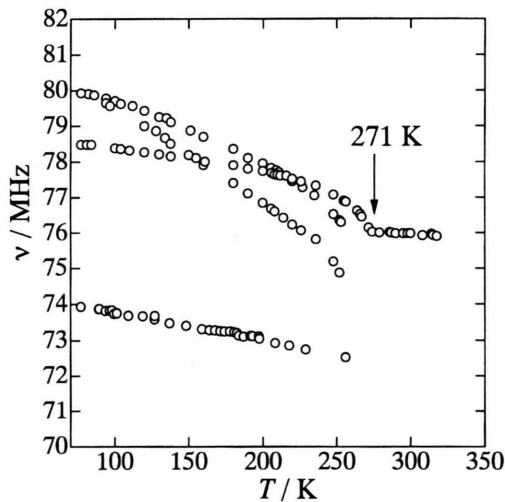

Fig. 8. Temperature of ^{81}Br NQR frequencies of bis(trimethylsulphonium) tetrabromocadmate(II).

with the $[(CH_3)_4N]^+$ cations having two potential minima. On the other hand, Asahi and *et al.* concluded that both anions and cations are disordered above the transition point [10]. The observed crystal structure of the room temperature phase of $[(CH_3)_4N]_2CdBr_4$ [10] shows that the Cd-Br(1) bond is almost parallel to the *c*-axis in space group Pmcn. Under the assumption that the $[CdBr_4]^{2-}$ tetrahedra rotate around the *c*-axis more easily than around the other axes, the electric field gradient (EFG) at the Br(1) site is little affected, while the EFG's at the

other three bromine sites fluctuate more, making three NQR lines disappear below the transition point. In $[(CH_3)_4N]_2ZnBr_4$ in the room temperature phase (phase I, $T_{1\leftrightarrow II} = 288$ K [13]), L_{11} is about two times higher than L_{22} and L_{33} (L_{ii} are the components of the librational tensor **L** in the rigid body analysis of the $[ZnBr_4]^{2-}$ tetrahedron) [14] and L_{11} is also higher than the others even in the low temperature phase [14]. This suggests that the $[ZnBr_4]^{2-}$ tetrahedron executes rotation with large amplitude around the Zn-Br(1) axis, i.e., nearly along the *a*-axis in the crystal space group Pnma. This explanation probably holds in the case of (**3**), because (**3**) shows the same ferroelastic transition with Pmcn $\leftrightarrow$ P2$_1$/c sequence (or Pnma $\leftrightarrow$ P2$_1$/a sequence) as $[(CH_3)_4N]_2$ ZnBr$_4$ [10, 13].

$[(CH_3)_3S]_2CdBr_4$ (**4**) shows four ^{81}Br NQR lines between 77 and 304 K. All NQR lines disappear above 304 K, as shown in Figure 8. The DSC measurement between 130 K and the melting point of 508 K showed phase transitions at 304 K (the temperature hysteresis was 11 K and $\Delta S = 46.8$ J K^{-1} mol^{-1}) and 501 K on heating, and (**4**) decomposes at the melting point. The NQR and DSC results suggest that the phase transition at 304 K is of first-order. The considerably large transition entropy suggests that the phase transition at 304 K is accompanied by a large scale disordering of cations and/or anions in the crystal.

Discussion

$[H_3N(CH_2)_3NH_3]CdI_4 \cdot 2H_2O$ (**1**) forms tetrahedral anions, while a perovskite layer structure is detected for $[H_3N(CH_2)_3NH_3]CdBr_4$ [3] and $[H_3N(CH_2)_3NH_3]CdCl_4$ [4]. Although $Cd_2I_6^{2-}$, composed of two edge-sharing CdI_4 tetrahedra, was found [15], it seems that the bridging power of the halogen atoms in the Cd complex is in the order Cl, Br > I. $[(CH_3)_4N]_2CdBr_4$ (**3**) and $[(CH_3)_3S]_2CdBr_4$ (**4**) crystallize with cations without hydrogen atoms to form hydrogen bonds of $N\cdots Br$ or $S\cdots Br$ and $[H_3CNH_2(CH_2)_3NH_3]CdBr_4$ (**2**) with a cation in which the methyl group prevents the formation of hydrogen bonds. All of them show the tetrahedral anion struc-ture. In addition, the number of hydrogen bonds of $N\cdots I$ in (**1**) is insufficient, because of the presence of the water molecules. These results suggest that hydrogen bonds play an important role in the formation of the condensed anion structure and that the proper number of hydrogen bonds is necessary for the formation of the perovskite layer structure [1, 2].

[1] H. Ishihara, S. Dou, K. Horiuchi, V. G. Krishnan, H. Paulus, H. Fuess, and Al. Weiss, Z. Naturforsch. **51a**, 1027 (1996).
[2] H. Ishihara, S. Dou, K. Horiuchi, V. G. Krishnan, H. Paulus, H. Fuess, and Al. Weiss, Z. Naturforsch. **51a**, 1216 (1996).
[3] H. Ishihara, S. Dou, K. Horiuchi, H. Paulus, H. Fuess, and Al. Weiss, Z. Naturforsch. **52a**, 550 (1997).
[4] R. D. Willett, Acta Crystallogr. Sect B **33**, 1641 (1978).
[5] G. M. Sheldrick, SHELX86. Program for the solution of crystal structures, University of Göttingen, Germany 1986. SHELX93. Program for crystal structure determination, University of Göttingen, Germany 1993.
[6] Further information of the crystal structure determinations may be obtained from the Fachinformationszentrum Karlsruhe, Gesellschaft für wissenschaftlich-technische Information mbH, D-76322 Eggenstein-Leopoldshafen, Germany. Inquiries should be accompanied by the depository number CSD-408644 (**1**) of CSD-408626 (**2**), the names of the authors and the full literature references.
[7] A. Bondi, J. Phys. Chem. **68**, 441 (1964). L. Pauling, The Nature of the Chemical Bond. 3rd ed., Cornell University Press, Ithaca, New York 1960. Al. Weiss and H. Witte, Kristallstruktur und chemische Bindung. Verlag Chemie, Weinheim 1983.

[8] MO calculations were performed with the MOPAC93 programm: J. J. P. Stewart, Fujitsu Limited, Tokyo, Japan 1993. Geometry optimization was performed with the PM3 and EF method. The all *anti* conformer is the most stable one. The conformer in the crystal is less stable by 16.25 kJ mol^{-1} than the all *anti* conformer.
[9] S. Sato, R. Ikeda, and D. Nakamura, Bull. Chem. Soc. Japan **59**, 1981 (1986).
[10] T. Asahi, K. Hasebe, and K. Gesi, J. Phys. Soc. Japan **61**, 1590 (1992).
[11] H. Terao, T. Okuda, K. Yamada, H. Ishihara, and Al. Weiss, Z. Naturforsch. **51a**, 755 (1996).
[12] R. Perret, Y. Beaucamps, G. Godefroy, P. Muralt, M. Ehrensperger, H. Arend, and D. Altermatt, J. Phys. Soc. Japan **52**, 2523 (1983).
[13] K. Gesi and K. Ozawa, J. Phys. Soc. Japan **52**, 2440 (1983).
[14] P. Trouélan, J. Lefebvre, and R. Derollez, Acta Crystallogr. **C40**, 386 (1984). P. Trouélan, J. Lefebvre, and R. Derollez, Acta Crystallogr. **C41**, 846 (1985).
[15] P. L. Orioli and M. Ciampolini, J. Chem. Soc. Chem. Commun. **1972**, 1280.